

58/2-10-95 YS(2)

PREPARED FOR THE U.S. DEPARTMENT OF ENERGY,
UNDER CONTRACT DE-AC02-76-CHO-3073

PPPL-3034
UC-420,426

PPPL-3034

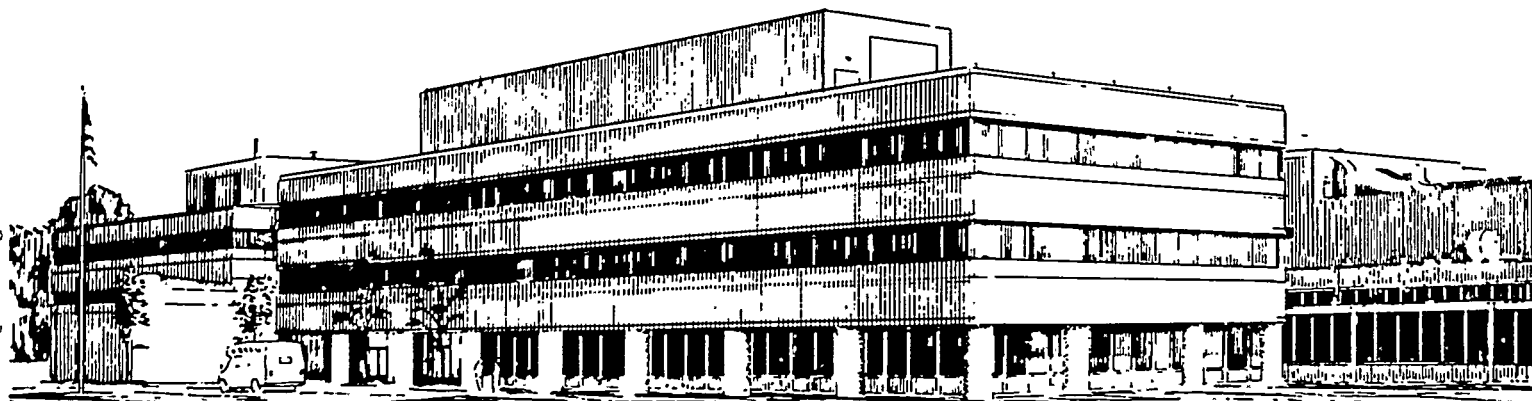
DESIGN STUDIES FOR ITER X-RAY DIAGNOSTICS

BY

K.W. HILL, M. BITTER, S. VON GOELER AND H. HSUAN

JANUARY 1995

PPPL PRINCETON
PLASMA PHYSICS
LABORATORY



DISTRIBUTION OF THIS DOCUMENT IS UNLIMITED

PRINCETON UNIVERSITY, PRINCETON, NEW JERSEY

NOTICE

This report was prepared as an account of work sponsored by an agency of the United States Government. Neither the United States Government nor any agency thereof, nor any of their employees, makes any warranty, express or implied, or assumes any legal liability or responsibility for the accuracy, completeness, or usefulness of any information, apparatus, product, or process disclosed, or represents that its use would not infringe privately owned rights. Reference herein to any specific commercial produce, process, or service by trade name, trademark, manufacturer, or otherwise, does not necessarily constitute or imply its endorsement, recommendation, or favoring by the United States Government or any agency thereof. The views and opinions of authors expressed herein do not necessarily state or reflect those of the United States Government or any agency thereof.

NOTICE

This report has been reproduced from the best available copy.
Available in paper copy and microfiche.

Number of pages in this report: 36

DOE and DOE contractors can obtain copies of this report from:

Office of Scientific and Technical Information
P.O. Box 62
Oak Ridge, TN 37831;
(615) 576-8401.

This report is publicly available from the:

National Technical Information Service
Department of Commerce
5285 Port Royal Road
Springfield, Virginia 22161
(703) 487-4650

DISCLAIMER

Portions of this document may be illegible in electronic image products. Images are produced from the best available original document.

Design Studies for ITER X-Ray Diagnostics*

K. W. Hill, M. Bitter, S. von Goeler, and H. Hsuan

Princeton Plasma Physics Laboratory
Princeton University
P. O. Box 451
Princeton, NJ 08543

* Supported by U.S. Department of Energy Contract Number
DE-AC02-76-CHO-3073

MASTER

MP

~~D~~ISTRIBUTION OF THIS DOCUMENT IS UNLIMITED

Abstract

Concepts for adapting conventional tokamak x-ray diagnostics to the harsh radiation environment of ITER include use of grazing-incidence (GI) x-ray mirrors or man-made Bragg multilayer (ML) elements to remove the x-ray beam from the neutron beam, or use of bundles of glass-capillary x-ray "light pipes" embedded in radiation shields to reduce the neutron/gamma-ray fluxes onto the detectors while maintaining usable x-ray throughput. The x-ray optical element with the broadest bandwidth and highest throughput, the GI mirror, can provide adequate lateral deflection (10 cm for a deflected-path length of 8 m) at x-ray energies up to 12, 22, or 30 keV for one, two, or three deflections, respectively. This element can be used with the broad band, high intensity x-ray imaging system (XIS), the pulse-height analysis (PHA) survey spectrometer, or the high resolution Johann x-ray crystal spectrometer (XCS), which is used for ion-temperature measurement. The ML mirrors can isolate the detector from the neutron beam with a single deflection for energies up to 50 keV, but have much narrower bandwidth and lower x-ray power throughput than do the GI mirrors; they are unsuitable for use with the XIS or PHA (except for narrow-band impurity monitoring), but they could be used with the XCS; in particular, these deflectors could be used between ITER and the biological shield to avoid direct plasma neutron streaming through the biological shield. Graded-d ML mirrors have good reflectivity from 20 to 70 keV, but still at grazing angles (<3 mrad). The efficiency at 70 keV for double reflection (10 percent), as required for adequate separation of the x-ray and neutron beams, is high enough for PHA requirements, but not for the XIS. Further optimization may be possible. The glass-capillary bundles have measured gains (x-ray / geometrical throughput) of 100 - 150 in the range 4-10 keV, but are probably not useful above 15 keV. They are compact and compatible with the XIS for low and medium frequency fluctuation measurements (tens of kHz), but may not be adequate for high frequency (>100 kHz) fluctuations. They are also compatible with Bragg survey spectrometers for impurity measurements, but not compatible with the Johann XCS used for ion-temperature measurement or with the PHA. The aperture sizes near ITER and near the x-ray optic, for instruments based on x-ray mirrors, are 10-20 cm² for an XIS channel, of order 10 cm² for the XCS, and 1 cm² for a PHA channel. The maximum radiation fluxes onto the x-ray optical element outside the biological shield are a few times 10⁹ to a few times 10¹⁰ cm⁻² s⁻¹ for 3000 MW operation, permitting lifetimes of several times 10³ to several times 10⁴ hours before radiation damage causes deterioration (assumed fluence 5 x 10¹⁷ to 10¹⁸ neutrons cm⁻²). An x-ray optic for the XCS located outside a 2-m thick shield/collimator plug between ITER and the biological shield would experience radiation flux densities of 10¹¹ cm⁻² s⁻¹, limiting its life to a few thousand hours at full power. The XCS can also function without an additional x-ray deflector, since its detector is already well isolated from the neutron beam. The resolving power limitations for the Johann focusing error and for deviation of the detector from the Rowland circle are estimated to be greater than 2.5

$\times 10^4$, for Krypton $K\alpha$ in first order reflection, implying that ion-temperature measurements are feasible.

I. Introduction

X-ray diagnostics provide a variety of types of information about tokamak plasmas.^{1,2} Arrays of broad energy bandwidth x-ray flux monitors (the X-ray Imaging System, or XIS)³ provide radial-profile information on MHD instabilities and other plasma fluctuations. The soft x-ray (1 - 100 keV) Pulse-Height-Analysis diagnostic (PHA)⁴ is a moderate energy resolution, moderate time resolution, broad band spectrometer which records an overview of the soft x-ray spectrum and can measure electron temperature, and measure low and medium-Z impurity concentrations. Higher energy (0.05 - 1.0 MeV) PHA systems provide information on non-thermal electron distributions.⁵ The X-ray Crystal Spectrometer (XCS) measures the ion temperature from Doppler broadening of impurity lines, usually $K\alpha$ lines of intrinsic metals, but also trace amounts of gases such as argon or krypton can be used.⁶ The XCS must have very good energy resolution, usually $E/\Delta E > 7000$.⁷ All of these conventional x-ray diagnostics are highly susceptible to background noise from interactions of neutrons and/or secondary gamma rays in the detectors; they require extensive radiation shielding,⁸ even under high power DD operation (deuterium neutral-beam heated deuterium plasmas). The PHA and XIS are virtually unusable at near-breakeven DT (deuterium + tritium plasmas and/or neutral beams) fusion conditions. Not only are the radiation noise levels much too high, but the silicon or germanium detectors would be quickly damaged by the neutron fluxes anticipated from ITER. The XCS, if properly positioned and shielded,^{9,10,11} can tolerate much higher neutron emission levels than can the other two diagnostics, since the detector is not in the line of sight; it measures x rays diffracted from a Bragg crystal.

Since standard tokamak x-ray diagnostic techniques are generally non-workable on ITER because of the high nuclear radiation background,¹¹ the present studies have focused on adapting these diagnostics to ITER by using additional x-ray optical elements to deflect the x-ray beam out of the neutron beam from ITER, or to reduce the neutron flux onto the diagnostic while maintaining high x-ray throughput. Preliminary studies of this type were presented in Ref. 11. Also, a companion report discusses in more detail radiation hardening of the XIS type of diagnostic.¹² An alternative approach to using reflective x-ray optics for the PHA is the use of an alternative type of line-of-sight x-ray detector, the x-ray microbolometer.¹³ These detectors should have a much higher ratio of x-ray to neutron/gamma ray response than conventional detectors and a radiation-damage threshold a few orders of magnitude higher than that of the Si(Li) or high purity germanium detectors used in present PHA systems. This detector could potentially be used in the PHA without reflective optics and, perhaps, could replace the XCS because of its potential for high energy resolution.^{13,14} Improvements in count rate need to be achieved, probably by developing arrays,¹⁵ and theoretically achievable improvements in energy resolution¹³ would be necessary for these elements to replace the XCS.

The motivation for developing x-ray diagnostic capabilities on ITER is that significant problems exist with other types of instruments which also measure some of the parameters provided by the x-ray systems. For example, the CHERS (Charge-Exchange Recombination Spectroscopy) diagnostic for ion-temperature measurement requires neutral-beam injection (NBI), which is a large, expensive ancillary system. Furthermore, the CHERS system on TFTR has problems with low signal levels under some conditions; the problems due to beam attenuation will be greatly exacerbated on ITER due to the longer neutral-beam path lengths in the plasma and higher plasma densities. The XCS can measure ion temperature without NBI, as long as trace levels of a suitable impurity exist in the plasma. The impurity concentrations necessary (for krypton) have been shown to be both (1) non-perturbing in the plasma center and (2) the proper levels to provide the desired edge cooling to help control the energy release from the plasma. An additional benefit of the XCS is that it can also measure electron temperature and impurity charge-state distributions.

The x-ray PHA is the most convenient way to identify and measure the absolute concentrations of medium- and high-Z impurities in the center of the high-temperature plasma. The $K\alpha$ x-ray lines of all charge states through He-like of an element are combined in a single peak at a well-defined energy and are generally emitted from the plasma core; UV and visible lines, however, generally come from the edge, and the spectra are more complicated and lines more difficult to identify. Furthermore, the PHA can accurately measure electron temperature. The laser-scattering electron-temperature diagnostics will suffer from radiation-damage of the optical vacuum windows, and electron-cyclotron-emission (ECE) diagnostics may have some technical problems with measurement in the high magnetic fields in ITER. The x-ray diagnostic channels described in this report are assumed to have a vacuum path to the vicinity of the first optical element, where the radiation fluxes are reduced relative to those near the first wall. A vacuum window of beryllium located at this point should have a lifetime of thousands of hours of operation at full power (assuming a damage threshold of $5 \times 10^{17} \text{ n cm}^{-2}$).

The XIS-type diagnostic is widely used to study fluctuations and obtain information on magnetic-field structure via tomography. It is sensitive to both electron density and temperature fluctuations; the two types of fluctuations can be readily separated by use of two detectors with different absorber foils. In addition a multichordal XIS can provide fast radial profiles of electron temperature without the technical problems encountered by the ECE systems or the window darkening difficulties associated with the laser-scattering diagnostic. The XIS system can also measure radial profiles of Z_{eff} ,¹⁶ and in this capacity does not suffer from problems associated with reflections or emission from the walls as does the visible-bremsstrahlung diagnostic.

To orient the reader, the radial locations of the ITER plasma and various shield walls are illustrated schematically in Fig. 1. Also shown is one

concept for a curved x-ray crystal spectrometer for ion-temperature measurement. The edge of the plasma is located about 11 m from the machine centerline. Immediately outside the vacuum vessel is the blanket, which absorbs much of the power from the fusion neutrons and protects the toroidal-field coils from neutron damage; in the midplane the blanket is about 0.8 m thick. The first defining aperture for the x-ray diagnostics and for the escaping fusion neutron beam would be a small penetration through this blanket and through a shield plug located just outside the vacuum vessel. The second defining aperture for the x-ray and neutron beams is the 2-m thick biological shield, beginning at 18 m from the centerline.

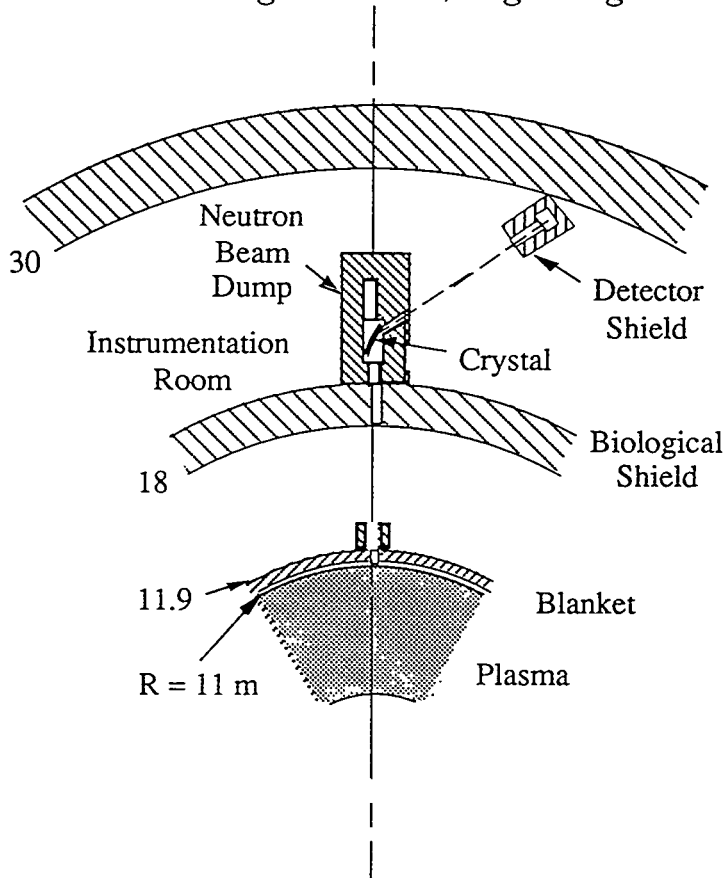


Fig. 1 Vertical-view schematic of ITER, surrounding shielding, and instrumentation room.

The radiation levels in the instrumentation room between the biological shield and the outer shield wall, which separates the instrumentation room from peripheral equipment rooms are low enough to allow survival of instrumentation during operation and personnel access between shots. The x-ray diagnostics might be located either in the instrumentation room or beyond the instrumentation room in the outer rooms, where the radiation fluxes are still lower.

The present study demonstrates that the three types of x-ray diagnostics, ion-temperature and plasma-motion measurement by x-ray crystal spectroscopy, fluctuation studies by high throughput x-ray

imaging, and plasma impurity monitoring and electron-temperature measurement by broad-band x-ray spectroscopy are, in principle, workable on ITER. Penetration requirements in the shielding near ITER are modest; the aperture needs to be of order 1 cm^2 for broad-band x-ray spectroscopy and of order $1 \times 10 \text{ cm}^2$ for an XIS or XCS chord. The XIS requires additional x-ray optics. The PHA with present Si(Li) and Ge detectors could be adapted with additional optics; or with further development for higher

count rates, the PHA function could be achieved by systems using x-ray microbolometer arrays either with or without additional optics. The XCS can be used directly on ITER with proper design and shielding; alternatively, one could also use additional optical elements to reduce the neutron flux onto the crystal and into the instrumentation room, or one could potentially replace the XCS by x-ray microbolometer arrays if improvements in energy resolution are achieved. This report discusses the design concepts and results of intensity calculations. In section II the types of x-ray optical elements considered are discussed. In section III possibilities for the XIS are summarized; a more detailed discussion is presented in Ref. 12. Section IV treats the XCS diagnostic. In section V broad band x-ray spectroscopy, in particular using the PHA type of diagnostic, is discussed. Finally, the results are summarized in section VI.

I. X-Ray Optical Elements

The key requirements for x-ray optical elements are that they (1) have sufficient reflectivity in the x-ray energy range of interest, (2) have adequate bandwidth, (3) provide the required reduction in background radiation signals, and (4) are able to survive the incident neutron fluxes for long periods of operation. Three basic types of x-ray optical preselecting elements have been considered. These are (1) flat, grazing-incidence (GI) x-ray mirrors; (2) flat, high-throughput Bragg reflectors; and (3) glass

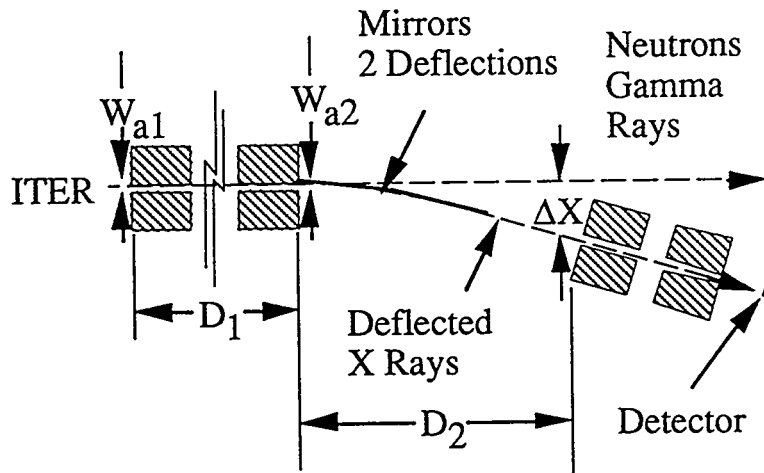


FIG. 2 Schematic of the grazing-incidence x-ray mirror concept for deflecting the x-ray beam from the neutron/gamma-ray beam from ITER. In this illustration two reflections are indicated.

capillary bundles which serve as x-ray "light pipes". The Bragg reflectors may be natural crystals or man-made multilayer (ML) elements, also sometimes called layered synthetic microstructures (LSM). We first briefly summarize the salient features of these optical systems.

The basic concept for the first two schemes is illustrated in Fig. 2. Two apertures of thickness sufficient to collimate the 14-MeV neutrons from ITER are placed one near ITER, and the other just in

from x-ray optical elements and sent to an exit collimator system which channels it to the detectors or spectrometer. The first aperture near ITER is an integral part of the first shield surrounding the ITER vacuum vessel, which reduces the radiation fluxes incident onto the toroidal field coils. The second aperture would probably be a part of the biological shield, which is located about six meters from the blanket and is two meters thick. The exit aperture system and detector or spectrometer can be located entirely in the instrumentation room, between the biological shield and the outer shielded rooms (See Fig. 1). Alternatively, the detector or spectrometer may be located in the outer shielded areas and a penetration through the outer shield wall may define part of the exit aperture system. Another alternative would be to locate the mirror between ITER and the biological shield, and use a narrow channel in a shield/collimator block, probably about 2 m thick, just outside the ITER port cover. This option, however, is likely to be feasible only for use of either multilayer mirrors or natural crystals to deflect the beam onto an XCS, since the broad bandpass GI mirrors would provide inadequate deflection at the high energies required by the XIS and PHA due to the short beam path available (4 m since 2 m of the available 6 m would be required for the shield/collimator block). The displacement Δx of the exit aperture from the path of the neutron beam must be sufficient to remove the aperture from the strongly forward-peaked cone of fast neutrons scattered from the mirrors entrance aperture, the mirror, and the supporting structure of the mirror.

The aperture near ITER is designed with an opening as small as possible and a length sufficient to minimize the neutron flux onto the x-ray optic and to minimize neutron/gamma-ray streaming into the instrumentation room. The neutron flux density at the optic is given by

$$\phi = \frac{B_n A_a}{D^2}, \quad (1)$$

where B_n is the neutron surface brightness across the viewing chord, A_a is the area of the aperture, and D is the distance from aperture to mirror. The central 14-MeV neutron surface brightness for ITER is estimated to be about $8 \times 10^{13} \text{ (cm}^2 \text{ s sr)}^{-1}$ for 3000 MW of DT neutrons, and we use a multiplier of 5 to estimate the total neutron emission including those which are downscattered one or more times inside the first shield. This type of enhancement has been predicted by Monte Carlo neutron transport codes for TFTR. These values are summarized in Table I, which list, among other things, the neutron brightness and neutron flux density at the crystal of the XCS. As an example, the neutron flux density at a mirror located 7 m from an aperture of dimensions 0.8 cm x 10 cm is $3 \times 10^9 \text{ n cm}^{-2} \text{ s}^{-1}$. If the neutron-damage threshold of the optic is $5 \times 10^{17} \text{ cm}^{-2}$, which is a reasonable estimate for mirrors and glass-capillary bundles, the lifetime of the optic would be 4×10^4 hours at full power. The exit aperture pair should also be designed with openings as small as possible consistent with functionality of the diagnostic, and the distance between the first exit

aperture and the second exit aperture, or the detector, should be as large as possible. The neutron or gamma-ray flux density streaming from the second exit aperture can also be estimated from Eq. 1 with B_n being replaced by the flux density of neutrons or gamma-rays scattered from the material in view of the detector; in the latter case, an angular dependence may be needed to account for the non-isotropic nature of the scattered radiation.

The GI mirrors rely on the high efficiency of metal or metal-coated glass surfaces for reflecting x rays by total external reflection when the x rays are incident at small angles, of the order of several milliradians.^{17,18}

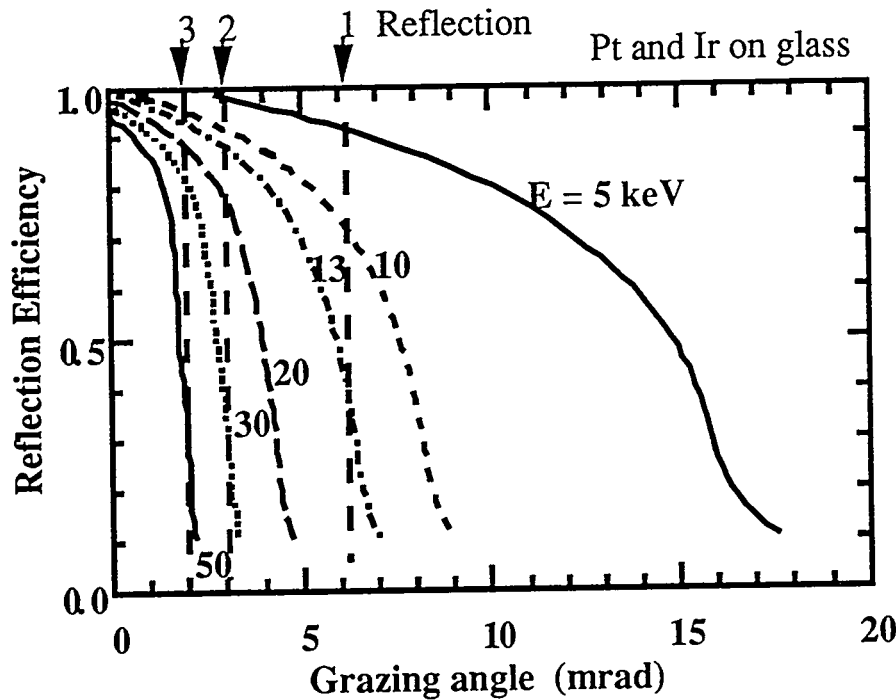


FIG. 3 Approximate reflectivity of x rays of various energies from platinum- and iridium-plated float glass surfaces as a function of the grazing angle of incidence relative to the surface. These curves were derived from an average parametric fit to data from Refs. 17 and 18.

The mirrors, typically flat float glass with an evaporated coating of a high-Z material, such as gold, platinum, or indium, have reflectivities of 90 percent or better for x rays striking at angles less than a critical angle θ_c measured relative to the surface. θ_c decreases with x-ray energy.

The reflection efficiency as measured in Refs. 17 and 18 is summarized as a function of grazing angle of incidence for several x-ray energies in Fig. 3. The vertical dashed lines point out the grazing angles

required to achieve a lateral deflection of 10 cm at a distance of 8 m from the mirrors for one, two, or three successive reflections; the corresponding maximum energies for good reflection efficiency are 12, 22, and 30 keV, respectively. Thus, the main advantage of the GI mirror is very broad bandwidth and, hence,

relatively high x-ray power throughput; we can realize acceptable isolation from the neutron beam over the entire x-ray band from the cutoff of any vacuum windows in the system up to 30 keV. This fact means that, for a reasonably sized mirror, intense signals can be measured, such as required

for ~ 100 kHz fast fluctuations; secondly, good throughput up to 30 keV implies that relatively thick, high-pass x-ray filters can be used to ensure that the intensity of the bremsstrahlung signal fluctuates significantly with small fluctuations in electron temperature, even for high electron temperatures (~ 20 -30 keV). The main disadvantages of GI mirrors result from the fact that the incidence angle for high reflectivity is small. Two consequences of this small angle are that (1) the total area of the mirror or mirrors must be large for usable signal, and (2) the amount of lateral deflection for a single reflection is small unless there is a very large distance between the mirror and the detector. This distance is expected to be about 8 m for ITER; thus, to achieve a lateral deflection of 10 cm with 1, 2, or 3 successive reflections, the grazing angle must be about 6, 3, or 2 mrad, respectively. From Fig. 3 we see that good reflectivity can be achieved for x-

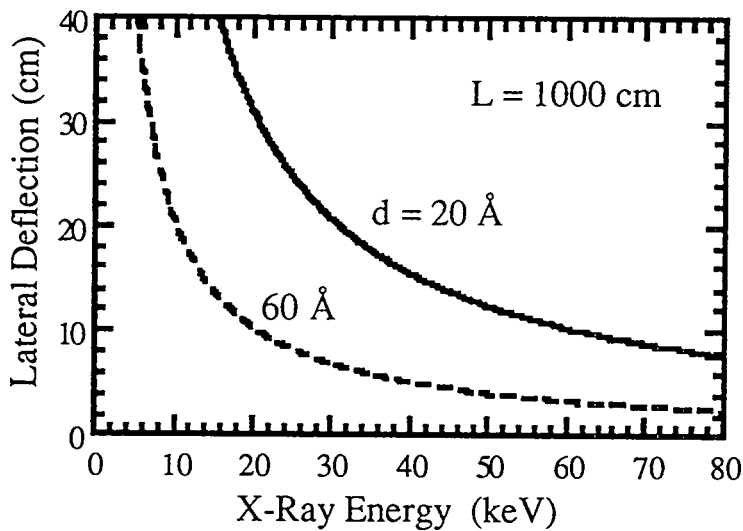


FIG. 4 Lateral deflection of an x-ray beam, relative to an undeflected ray, at a distance of 10 m from Bragg multilayer elements having $2d$ spacings of 40 and 120 Å, as a function of x-ray energy.

energy band of interest is large enough that a single reflection is adequate to remove the x-ray beam from the neutron beam, for the path lengths anticipated for ITER. Both natural crystals and man-made Layered Synthetic Microstructures (LSM) or MultiLayers (ML) can be used. The deflection is illustrated in Fig. 4 for multilayers having d spacings of 20 and 60 Å and a separation between ML and detector collimator of 10 m. The Bragg deflectors rely on Bragg diffraction of x rays from relatively high throughput natural or man-made metal multilayer "crystals". The high throughput is achieved by using elements with a broad rocking curve and reasonably high peak reflectivity.^{19,20} In general, Bragg elements may have good throughput over a limited energy band, whereas GI mirrors have good reflectivity over an extended energy range.

ray energies up to 12, 22, and 30 keV, respectively, for these three grazing angles. The lateral deflection of 10 cm was chosen to allow adequate removal of the x-ray beam from the streaming neutron beam since about 7 cm of deflection¹¹ from the neutron beam has been estimated to be sufficient to adequately reduce the fraction of neutrons scattered from the mirror into the diagnostic collimator.

The second type of mirror element, Bragg reflectors, have a major advantage in that the deflection angle for soft x rays over most of the

The main disadvantages of most high throughput Bragg elements are that (1) only a narrow band of x rays ($E/\Delta E \sim 50 - 100$ for ML and graphite crystals) is reflected at a given angle of incidence and (2) the peak x-ray reflectivity is typically only about 30-50 percent, somewhat lower than available with GI mirrors at angles less than the critical angle. (Exceptions are the recently-developed x-ray supermirror^{21,22}, or graded-d mirror, in which the layer spacing varies with depth and the bandwidth can be much broader than that of single-d multilayers, and some recently-developed multilayers which have reflectivities up to 70 percent.) These factors result in a throughput of x-ray power much lower than that of the GI mirror, so that single-d ML elements are less attractive for use with fast fluctuation diagnostics.²³ A more detailed comparison of the signals expected from the ML relative to those from the GI reflector in a XIS instrument is presented in Ref. 12. Roughly, the signal from a single ML mirror with uniform layer spacing is predicted to be about one percent of that for a GI mirror for a plasma with electron temperature of 10 keV. Also the narrow bandwidth makes uniform-layer-spacing ML preselectors unattractive for use with the broad band PHA spectrometer. However the narrow bandwidth is not a serious fault if the ML is used as a preselector for the XCS; either (1) the bandwidth can be broadened enough to pass the range of x-ray energies required for Doppler broadening measurements by using fewer layers (at the expense of a nominal decrease in reflectivity) or by varying the thickness of the layers with depth, or (2) the plane of the ML can be tilted slightly relative to the plane of the aperture at the tokamak.. This tilt can be chosen such that the angle of incidence of the x rays varies slightly along the ML, and, hence, the central wavelength diffracted varies with position along the mirror, as required by the Johann configuration of the XCS.⁶

Broadening of the bandwidth of multilayers has been studied both theoretically and experimentally for astrophysical applications, in particular for improving the intermediate- and high energy performance of nested-mirror x-ray telescopes. For example, studies indicated that the throughput of a telescope in the region around the iron K emission lines could be increased by a factor of 3 - 5 in a narrow band, or 1.3 - 2 in a broader band by replacing the outer reflectors of a GI telescope with appropriately tailored ML reflectors.²⁴ Also, measurements have shown that the bandwidth of graded-d multilayers can be a factor of about 2 - 2.5 times greater at 8 keV than the bandwidth of single-d multilayers at the expense of about a 10 percent reduction in peak reflectivity.²⁵ Very recently, even broader bandwidth graded-d "supermirrors"^{21,22} have been developed. A bent W/Si supermirror with x rays incident at 2.94 mrad exhibited an average reflectivity which decreased monotonically from about 60 percent near 15 keV to 30 percent at 70 keV; oscillations in both the theoretical and measured reflectivity with energy from about 35 percent to 70 percent were observed. Operationally these supermirrors would be more like GI mirrors than like multilayers because of the very small angles of incidence; however, these elements for the first time make it possible to consider performing x-ray measurements on ITER in the region above 50

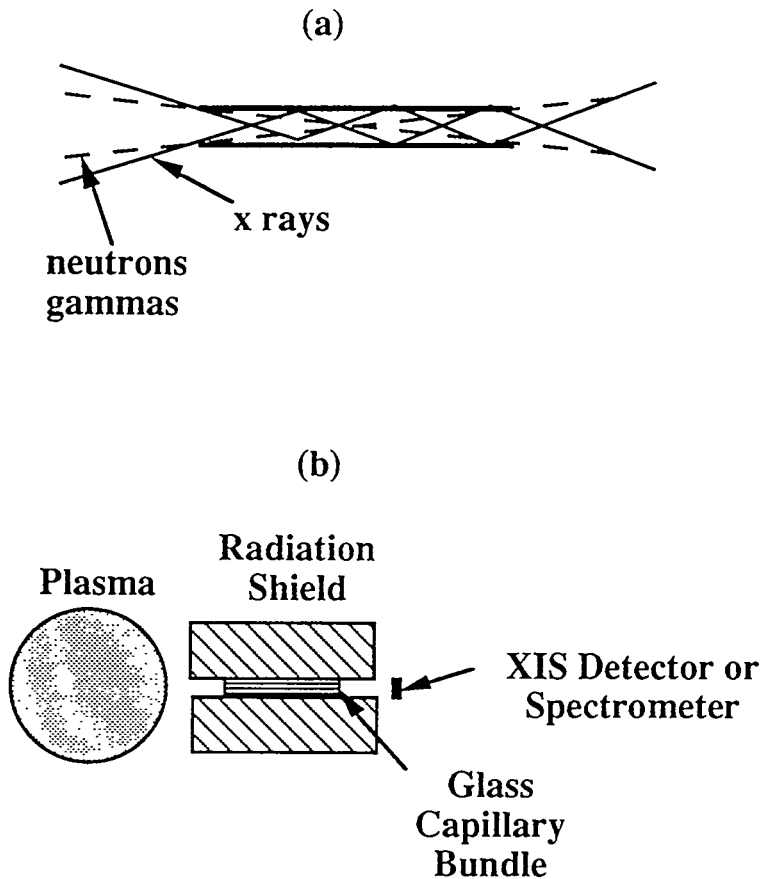


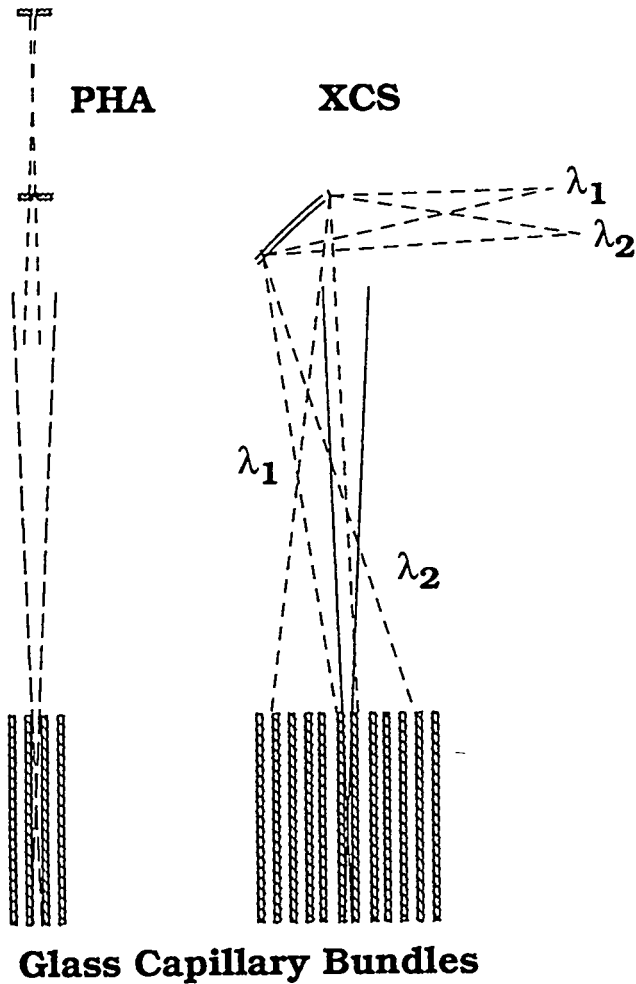
FIG. 5 (a) Illustration of the enhancement of x-ray solid angle of a glass capillary relative to the geometrical solid angle due to total external reflection of the x rays from the inner walls of the tube. (b) Use of bundles of capillaries to reduce neutron flux from plasma.

and gamma-ray transmission is assumed to be governed by the geometrical throughput. The measured relative gain of the best capillary bundle (x rays / neutrons) ranges from 110 to 150 in the x-ray energy range 4.5 to 10 keV. A second bundle has gains of 80 to 100 over the same range. One of these instruments has been installed on TFTR and is awaiting testing.²⁶ This is a relatively simple, direct concept with broad bandwidth and high throughput; but the technique may have limited usefulness at energies above 12 - 15 keV, and has lower radiation-noise rejection than that capable with GI mirrors or multilayers. It could be used as a preselector for impurity spectrometers, e. g., low or moderate-resolution Bragg monochromators or convex-crystal spectrometers, but is not compatible with conventional high-resolution curved-crystal spectrometers as used for ion-temperature measurement. This incompatibility is illustrated schematically in Fig. 6.

keV, which is important for plasmas with electron temperatures of 20 to 30 keV.

The third element, glass capillary x-ray "light-pipe" bundles, was developed mainly to address the issue of high throughput x-ray fluctuation measurements.²⁶ The concept of this element is illustrated in Fig. 5. The capillary bundle is embedded inside a penetration in a thick neutron shield, and the x rays (and neutrons) passing through the element are channeled to a shielded area where the x-ray signal can be measured by a detector or analyzed by a spectrometer. Because of grazing-incidence reflections from the walls of the glass tubes, the acceptance cone angle, or the numerical aperture for x rays is larger than the geometrical throughput of the capillary channels. The neutron

Furthermore the instrument designed for TFTR is not fully compatible with the standard soft x-ray PHA as used on TFTR because the PHA has some detector and aperture configurations which have smaller solid angles than that of the capillary channels. This idea is also illustrated in Fig. 6. Thus



Glass Capillary Bundles

FIG. 6 Illustration of the incompatibility of the glass capillary bundles with the x-ray PHA, because of the relatively smaller solid angle of the PHA, and with the XCS, because of the relatively large range of angles for incident x rays required by the XCS.

the basic concept of reducing the solid angle of the neutrons, as determined by the capillary length and diameter, to values smaller than that of the x rays is not fully achievable for the capillary-PHA combination. The PHA would be compatible with capillaries having a smaller diameter, for the same length, than that of the TFTR instrument, but the transmission efficiency would be lower because of a higher numbers of reflections. A second fault with the capillary-PHA combination is that the PHA is often used to measure the continuum spectrum up to 50 or 100 keV, and the capillaries are incapable of providing x-ray/neutron gain for energies above about 12-15 keV as indicated earlier. One potential advantage of the capillary bundles, relative to the x-ray mirrors is the small lateral size. The capillary bundles are about two cm in diameter; the apertures at ITER and at the detector would need to be about 6-7 cm in diameter, if the bundle were about 8 m from each aperture, due to the diverging entrance and

exit cones of the radiation. Thus, each channel requires a small cylindrical channel of real estate from the tokamak to the shielded detector room. The x-ray mirrors will likely need to be

10 cm wide for XIS applications and will require 15-20 cm of space in the plane of the deflection. Thus, the capillary bundles are more convenient for closely-packed multichord x-ray imaging. Another favorable aspect of the capillary bundle is the fact that, once a bundle is fabricated and characterized, the throughput as a function

of x-ray energy is known, whereas the transfer function of the GI and ML mirrors will be a more sensitive function of the alignment, which must be performed and characterized in the field.

III. X-Ray Imaging System

The x-ray imaging arrays can be used to measure a variety of plasma parameters. These include high frequency (>50 kHz) fluctuations or instabilities, MHD phenomena, sawtooth behavior, electron-temperature profiles, impurity transport, and Z_{eff} profiles. One of the most important applications is the study of fast fluctuations, because these phenomena are thought to be related to particle and energy transport. Studies on adapting the conventional XIS array for use on ITER were done first for two reasons: (1) it is an important basic diagnostic for studying MHD activity and fluctuations, which is crucial for understanding stability and transport; and (2) the XIS has a high sensitivity to radiation noise because it requires high x-ray fluxes and, hence, experiences high neutron fluxes if the detectors view the plasma directly. We will begin with a discussion of the use of glass capillary bundles to radiation harden the XIS. Neutron and x-ray throughput

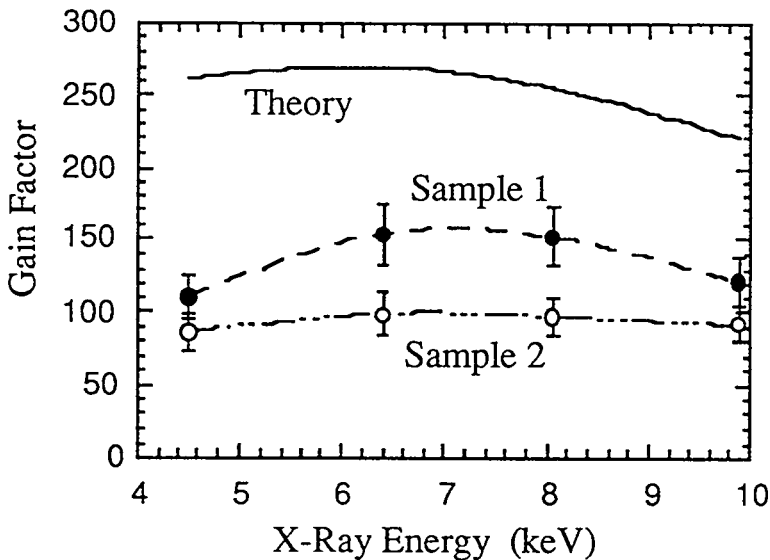
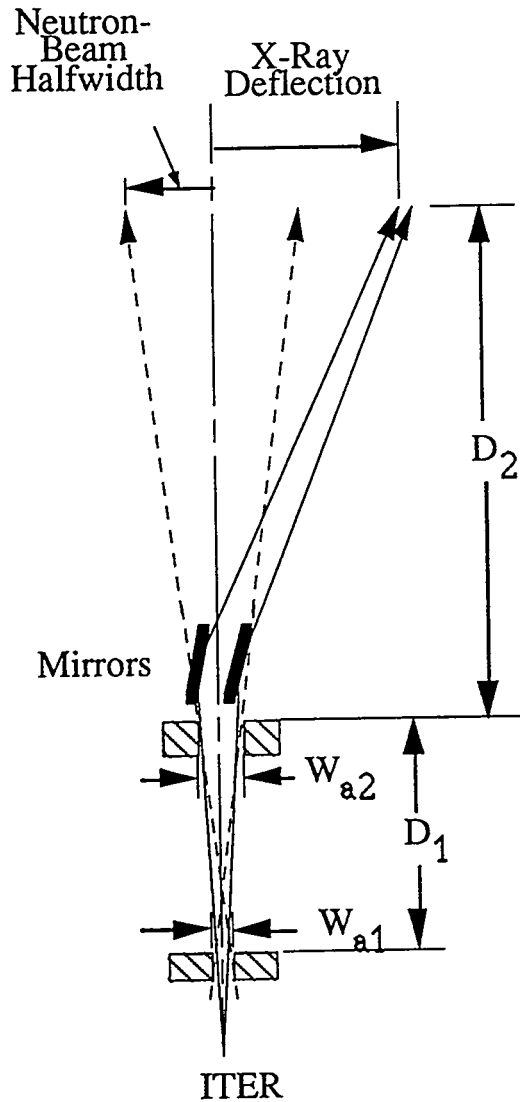


FIG. 7 Theoretical and measured x-ray transmission and gain ratio (ratio of x-ray solid angle times reflection efficiency to geometrical solid angle) for two glass capillary bundles of length 70 cm, as a function of x-ray energy. From A. S. Krieger.

calculations were done for a glass capillary bundle embedded in a channel in a neutron/gamma shield. The results suggested that for 30 MW of DT fusion neutrons from TFTR, a 70-cm long, 2-cm diameter bundle of straight glass capillaries with 50 percent packing fraction would suffice to reduce the radiation background signal in a typical XIS detector to the desired value of 1 nA while still passing the same x-ray intensity as each channel of the TFTR horizontal XIS array. The ideal theoretical gain was predicted to be about 270 at 6 keV. Such glass capillary bundles were developed and carefully

characterized for x rays at energies ranging from 4 to 10 keV. ²⁶ Arrays of

different lengths from 20 cm to 80 cm were tested to verify the scaling of a theoretical model. The measured throughput of the best 70-cm array was about 60 percent of the ideal theoretical throughput. The theoretical gain (ratio of measured x-ray transmission to the geometrical throughput) is shown in Fig. 7 as a function of x-ray energy for two 70-cm-long capillary-bundle samples. Thus the glass capillary bundle concept offers the possibility of enabling fast fluctuation measurements on ITER by improving the signal to noise ratio by a factor of 100 or better. One such capillary bundle has been installed on TFTR and is awaiting evaluation under DT conditions.



The second XIS concept for fast fluctuations considered involved using flat, grazing-incidence x-ray mirrors. For a single GI mirror located 6 m from the first ITER aperture to provide the same throughput as a TFTR XIS channel, the mirror would need to be, e. g. about 1 m long and 20 cm wide and be illuminated by x rays from a 1 cm x 20 cm aperture (in a neutron shield) at ITER. To reduce the size of the first aperture and the length and width of the mirror, stacked arrays of 5 mirrors, e. g. spaced a few mm apart, with dimensions of 40 cm in length and 10 cm in width could be used with a 0.8 x 10 cm² first aperture (See Table I). The stacked-mirror configuration has been used for x-ray telescopes;²¹ the concept is depicted in Fig. 8, where only two mirrors are shown for illustrative purposes. These smaller arrays of mirrors could then be enclosed in small vacuum housings and the x rays could be conducted to and from the reflective elements via standard 4 inch diameter vacuum plumbing. Again, at least two reflections would be required for energies above about 15 keV because of the grazing angles. The intensity of x rays reflected from the mirror or mirror array was calculated from the equation

$$I = B \frac{A_a A_m \sin \theta}{D^2} \eta \quad (2)$$

FIG. 8 Concept for using stacked multiple x-ray mirrors to deflect the x-ray beam away from the direct neutron beam.

where B is the surface brightness of x rays emitted from the plasma in the line of sight viewed by the mirror, A_a is the area of the aperture nearest ITER, θ is the angle between the incidence rays and the plane of the mirror, A_m is the total area of the mirror array, D is the distance from the first aperture to the mirror, and η is the efficiency for reflection of the x rays from the mirror. This efficiency is summarized in Fig. 3.

Details of a calculation of throughput for a 5-mirror ITER XIS channel based on Eq. 2 are given in Ref. 12. The dimensions and parameters of this design are summarized in Table I, taken from Ref. 12.

Table I. Dimensions and other physical parameters of a 5-mirror, single deflection x-ray imaging channel optimized at an x-ray energy of 13 keV.

Parameter	Units	Quantity
Distance ITER to mirror	cm	700
Distance mirror to exit collimator	cm	1000
First aperture width	cm	0.8
First aperture height	cm	10
Second aperture width	cm	1.8
Mirror height	cm	10
Mirror length	cm	40
Number of mirrors		5
Neutron-beam lateral half width	cm	2.8
Grazing angles	mrad	3.7 - 5.5
Lateral x-ray deflection	cm	8.8 - 9.6
Reflection efficiency at 13 keV, η		0.7
TFTR minor radius	cm	90
ITER minor radius	cm	280
$V\Omega$ for TFTR	$\text{cm}^3 \text{sr}$	0.028
$\eta \times V\Omega$ for ITER	$\text{cm}^3 \text{sr}$	0.058
Fusion neutron power	MW	3000
Neutron surface brightness x 5	$\text{cm}^{-2} \text{s}^{-1} \text{sr}^{-1}$	2.5×10^{14}
Neutron flux density at mirror	$\text{cm}^{-2} \text{s}^{-1}$	3×10^9
Neutron radiation-damage threshold	n cm^{-2}	5×10^{17}
Mirror lifetime	hr	4×10^4

This design provides an effective throughput twice that of the TFTR horizontal XIS array. The higher throughput compensates for the lower photon statistics of the higher energy x rays expected to be used on ITER (relative to the energies used on TFTR) and the observation that the signals from the TFTR horizontal XIS are not optimal for fast fluctuation measurements. We see that the aperture and mirror dimensions are reasonably small, and the neutron flux density at the mirrors is low enough to allow an estimated 4×10^4 hours of operation at the 3000 MW DT neutron level before replacement of the mirrors.

The third technique, using uniform-layer-spacing multilayer diffracting elements for fast fluctuation measurements, has the disadvantage of much lower intensity than that available from the GI mirror for the same mirror and aperture sizes; recently-developed, broader-bandwidth ML mirrors may significantly increase the throughput of this type of system.^{21,22} The lower intensity prediction is based on both throughput calculations and on measurement results from such a system developed and tested on TFTR.²³ In the TFTR instrument an 8-element ML array was tuned to pass a bandwidth of about 1 keV, from 3 to 4 keV. The maximum measured current from the detector, which spanned about one-sixth of the beam area, was 35 nA. Even with a larger detector, the expected signal for a good TFTR supershot of about 200 nA is marginal. For 500 kHz fluctuations one needs closer to a 1 μ A signal for 1 percent statistics. Furthermore, the $A\Omega$ product of the TFTR instrument, which would define the minimum neutron flux streaming through the openings in the ITER blanket, was much larger than that desirable for a system on ITER. This product is defined by the equation

$$A\Omega = \frac{A_a A_{\perp}}{D^2}, \quad (3)$$

where A_a is the area of the aperture at ITER, A_{\perp} is the area of the mirror projected onto a plane perpendicular to the direction of incident x rays, and D is the distance between the first aperture and the mirror. For the TFTR ML prototype system the $A\Omega$ product was about 25 times that of the GI mirror design of Table I.

Further optimization of ML mirror systems might lead to designs which are more competitive with those using GI mirrors. A detailed comparison of the calculated throughput of a ML system with that of a GI mirror system is given in Ref. 12. Briefly, the throughput limitation of ML mirrors is based on the requirement to satisfy the Bragg equation. If the aperture at ITER is small ($\sim 1 \times 10 \text{ cm}^2$), and the distance from the aperture is large ($\sim 6 \text{ m}$) to provide a narrow neutron beam and to minimize the neutron flux onto the mirror, then the range of angles of incidence of the x rays onto the ML mirror is small. In fact, this angular range is about

the same as the typical "rocking-curve" angular width of a single-d ML, about 0.1 - 0.15 degrees. Thus, the bandwidth $\lambda/d\lambda$ is of order 50 to 100, and the spectral intensity reflected, e. g. at an x-ray energy of 10 keV, is only of order one percent of the total bremsstrahlung intensity from 4 to 20 keV for an electron temperature of 10 keV. Thus, the graded-d multilayers, or supermirrors, which show good reflectivity over an extended band, e. g., from 15 to 70 keV, may offer significant improvement over the single-d mirrors. We have not attempted to model the performance of an XIS based on graded-d reflectors in this report, but such an analysis should be done in future work.

IV. X-Ray Crystal Spectrometer

Adaptation of the high-resolution x-ray crystal spectrometer (XCS) to ITER was studied because of the importance and difficulty of measuring the ion temperature on ITER. The studies involved MIST simulations to determine which impurity element will not burn out at high ITER temperatures,¹¹ measurement of lines from the selected element (krypton) on TFTR,^{27,28} calculations of signal and radiation noise for an XCS which views ITER directly, and calculation of throughput of a flat GI mirror as a preselector combined with an XCS located in a radiation-free area. The measurements on TFTR showed that heliumlike Kr lines can be used for T_i measurements. These measurements along with measurements of radiated power, combined with MIST simulations of Kr x-ray emission and radiated power showed that small, unperturbing concentrations ($\sim 10^{-4} \times n_e$) of Kr could be used for T_i measurements on ITER while also providing the desired feature of controlling the release of energy in the form of radiation from the plasma edge. The present study shows also that defocusing errors associated with the Johann geometry at small Bragg angles (28 degrees for the ITER design) are not large enough to prevent ion-temperature measurement; these errors remain manageable because of the small ratio of crystal length to focal length and the small detector length.

The intensities of the x-ray line and the background nuclear radiation noise for the direct-viewing XCS were based on the concept illustrated in Fig. 1. The x-ray and neutron/gamma-ray count-rate calculations are summarized in Table II. The x-ray intensity calculations were based on the equation

$$I = \frac{B \epsilon R_c h_a A \sin(\theta)}{D} \quad (2)$$

where I is the number of counts in the detector per second; B is the surface brightness of x-ray photons emitted from the plasma; ϵ is the detector efficiency; R_c is the integrated reflectivity of the crystal; h_a is the

height of the aperture near the plasma in the direction perpendicular to the
Table II Dimensions, intensities, and other parameters for an ITER curved
x-ray crystal spectrometer.

Parameter	Units	Option 1	Option 2
Distance aperture to crystal	cm	800	2000
Aperture height	cm	1	1
Aperture width	cm	7	10
Crystal width	cm	1	1
Crystal length	cm	12	20
Bragg angle	deg	28	28
Crystal 2d spacing	Å	2.028	2.028
Integrated reflectivity	rad	$5 \cdot 10^{-6}$	$5 \cdot 10^{-6}$
$\lambda/\Delta\lambda$ (Johann)		$3.5 \cdot 10^4$	$6 \cdot 10^4$
$\lambda/\Delta\lambda$ (Off Rowland Circle,.001)		$2.4 \cdot 10^4$	$3.2 \cdot 10^4$
Central electron temperature	keV	20	20
Central electron density	10^{20} m^{-3}	1.1	1.1
Krypton concentration		$1 \cdot 10^{-4}$	$2 \cdot 10^{-4}$
Kr contribution to Z_{eff}		0.13	0.26
He-like Kr brightness	$(\text{cm}^2 \text{ sr s})^{-1}$	$1 \cdot 10^{13}$	$2 \cdot 10^{13}$
Krypton count rate	s^{-1}	$3.5 \cdot 10^5$	$5 \cdot 10^5$
Kr radiated power	MW	40	80
Fusion neutron power	MW	3000	3000
Neutron brightness x 5	$(\text{cm}^2 \text{ sr s})^{-1}$	$4 \cdot 10^{14}$	$4 \cdot 10^{14}$
Neutron flux at crystal	$\text{cm}^{-2} \text{ s}^{-1}$	5×10^{10}	2×10^{10}
Crystal damage threshold	cm^{-2}	5×10^{17}	5×10^{17}
Life of crystal	hours	2600	7000
Neutron scattering prob.		0.3	0.3
Detector eff. for radiation		0.15	0.15
Scattering enhancement		x 2	x 2
Radiation count rate	s^{-1}	1100	640
Bremsstrahlung count rate	s^{-1}	2×10^5	8×10^4

plane of dispersion; A is the crystal area; θ is the Bragg angle (angle between incident ray and surface of crystal); and D is the distance from the plasma aperture to the crystal. The brightness of Kr photons at the plasma surface was calculated by the MIST code.¹¹ The brightness of neutron and gamma-ray emissivity from the aperture was based on a 14-MeV neutron source strength of 3000 MW increased by a factor of 5 to account for enhancement due to multiply scattered neutrons and production of secondary gamma rays inside the ITER first shield. This enhancement factor is typical for that calculated by neutron/gamma-ray transport codes for TFTR with a two-foot-thick "igloo" shield surrounding the tokamak. A factor of 2 enhancement, relative to isotropic scattering, of neutrons scattering from the crystal structure was assumed. The average detector efficiency for radiation of 15 percent is based on TFTR measurements and predictions of radiation flux by a neutron/gamma-ray transport code (10 percent efficiency with a safety factor). Two effects which have not yet been calculated for this design are (1) the effectiveness of the radiation dump for absorbing nuclear radiation escaping from the biological shield, and (2) the dimensions of the detector shield and collimator required to reduce the radiation noise to acceptable levels. These quantities will be calculated once the radiation fluxes due to transport through the biological shield are known.

The radiation background levels were rigorously calculated for a design presented by Bryzunov.²⁹ In this design the spectrometer was located inside the ITER instrumentation room. The x rays and neutrons were conducted through a $8 \times 12 \text{ cm}^2$ penetration in the ITER blanket/shield. This penetration is much larger than that considered for the XCS designs in this work. A $4 \times 60 \text{ cm}^2$ cylindrical graphite crystal was used to deflect the x-ray beam to an 8-cm diameter quartz crystal with a spherical surface curvature, located outside of the neutron beam. Focusing by the spherical crystal allowed use of a small detector cross section and a reduced penetration cross section at the biological shield. The background levels allowed ion-temperature measurement as long as the x-ray count rate was kept greater than 10^5 s^{-1} when the neutron source strength from ITER was about one third that considered in Table II (1 MW m^{-2} vs. 3000 MW or about 3.5 MW m^{-2}). Although the choice of aperture and crystal sizes depends on the assumptions of plasma size, krypton concentration, and other plasma parameters, which may have been different in this earlier design than in the present ITER configuration, the main point is that the background radiation noise was not deemed to be intolerable. Thus, it appears that our design may have acceptable signal to noise levels since our count rates are greater than 10^5 s^{-1} . It is expected that the radiation noise could be kept to much lower levels if the spectrometer were located outside the instrumentation room, beyond the third shield in Fig. 1, or if an x-ray deflector were used between ITER and the biological shield to avoid streaming of direct plasma neutrons through the biological shield.

Spectrometer designs using a spherically-bent crystal have also been considered by Bitter.³⁰ This approach may allow use of smaller apertures at

ITER and smaller detectors, which would reduce the requirements on the crystal and detector shield and beam dump. It is not clear, however, how much advantage spherical crystals would have over the present cylindrical crystals for the long distances considered in the present design.

The signal-to-noise ratio in the calculation of Table II is quite good. However, inherent in the calculation is an assumption of ideal shielding and collimation, i. e., that the only nuclear radiation which can reach the detector is that which is scattered directly from the crystal. From experience with TFTR it is known that radiation transported through radiation shields and streaming through penetrations in the shields for other diagnostics and subsystems always increases the background level well above ideal levels. If, in fact, the ambient radiation levels in the detector room should be significantly higher than that due to the radiation scattered from the crystal, it would be necessary to enclose the detector in an effective radiation shield with a penetration for the x rays, and, perhaps, to use an additional neutron/gamma-ray detector behind the x-ray detector and coincidence electronics to reject a portion of the radiation noise. The detector should be well shielded and collimated so that the background radiation is predominately parallel to the x-ray beam. The back wall of the detector should be thin and of a low-Z material, such as aluminum, and minimal electronics components should be located behind the detector; these features are to minimize the probability of the neutrons or gamma rays interacting in material behind the detector and producing secondary radiation which produces counts in the detector. If lead gamma-ray shielding is used, a graded-Z layer consisting of, e. g., copper and aluminum foils should be used between the lead and the detector to reduce noise due to fluorescence of lead and copper x rays. The probability of the neutrons and gamma rays of energy above about 200 keV interacting in the detector gas volume is small (about 5 percent).

Even for the small Bragg angles expected for krypton x rays of wavelength 0.93 Å (28 degrees for quartz 203 planes with $2d = 2.028$ Å), the focusing errors due to (1) the Johann crystal geometry²⁹ and (2) the deviation of a linear detector from the Rowland circle when the detector plane is perpendicular to the incident x rays are not a problem. Both errors increase with decreasing Bragg angle, increase with detector length, and decrease with crystal radius of curvature. For a crystal of length 12 cm and 16 m curvature radius the Johann error at a Bragg angle of 28 degrees limits the resolving power ($\lambda/d\lambda$) to about 35000. Similarly, the beam defocusing due to error (2) above at a point on the detector located about 4.3-cm from the Rowland circle limits the resolving power to about 24000. The net resolving-power limit due to the two focusing defects is well above the 7000 - 10000 required for accurate ion-temperature measurement. Moreover, the region of detector ± 4.3 cm from the Rowland circle is long enough to allow a bandwidth ($d\lambda/\lambda$) of about one percent. This bandwidth is sufficient to cover the full width, from 0.1 percent of peak height to 0.1 percent of peak height, of a Doppler-broadened Gaussian peak emitted by 50-keV krypton ions, which is about 0.6 percent, and also provide a region

of the spectrum for background subtraction. It was important to evaluate these focusing errors because of the small Bragg angle, 28 degrees; the Bragg angles for all T_i-measurement spectrometers at Princeton have been in the range 43 - 65 degrees, where the focusing errors are smaller.

Another ion-temperature measurement concept which might be suitable for ITER is that of the double-crystal scanning monochromator which is used on the JET (Joint European Torus) tokamak. The double x-ray reflection permits a labyrinth-geometry to shield the detector from the incoming radiation beam; the geometry also requires two reflections for the neutrons or gamma rays to reach the detector. In practice, however, the detector is physically much closer to the first crystal and to the neutron dump behind this crystal than is the case with the long focal-length, curved-crystal spectrometer; this situation implies a relatively higher susceptibility to radiation noise in the nearby detector due to the buildup of multiply scattered nuclear radiation inside this compact labyrinth. The situation is exacerbated by the smaller throughput of the flat-crystal instrument, which calls for larger areas for the crystal and the aperture near ITER in order to achieve the same time resolution as for the curved XCS; these larger areas result in higher neutron fluxes. A more thorough comparison of the relative susceptibility of the two instruments to radiation noise should be performed. An advantage of the flat-crystal scheme is that broader bandwidth can be achieved than for the curved XCS because of the relatively large range of Bragg angles which can be scanned. Also, selection of a different crystal to change the bandpass region is not as problematic as it is for the curved XCS; for the curved XCS, one may need to change the angle of the crystal-to-detector arm (and move the heavy detector shield) to measure the desired energy range. Thus, the two-crystal monochromator is better suited for lower resolution, broader band impurity monitoring. Two major disadvantages of the scanning monochromator as an ion-temperature diagnostic are that (1) the minimum integration time is of order 1 second, since the spectral line must be scanned, and (2) the two crystals must be moved linearly and rotated while keeping extremely small angular tolerances. Furthermore, the x-ray throughput is about 15 percent of that of a Johann system with the same aperture and crystal sizes due to the peak reflectivity of the second crystal and the transmission factor of the Soller collimator.¹⁰

As a possible alternative to the direct viewing XCS, the concept of using an x-ray optical preselector to avoid irradiating the crystal by the direct neutron beam was also studied. This concept is illustrated by Fig. 9. If the preselector were located in the region between ITER and the biological shield, it could prevent direct plasma-neutron streaming into the instrumentation room. However, in this region grazing-incidence mirrors are less suitable because a single reflection might not provide adequate lateral deflection for x-ray energies above about 5 keV. The reason is that the deflection arm can be only about 4 m long, since the distance between the ITER port and the biological shield is about 6 m, and a collimator of 2-m length just outside the ITER port would be required to restrict the lateral

spread of the neutron beam. If the grazing-incidence mirror considered earlier were located just outside the biological shield and coupled with the XCS system, it would be equivalent to an XCS having an entrance slit of width 0.5 cm in the direction perpendicular to the plane of dispersion. This is one half the width of that in the directly viewing XCS design of Table II. Thus, accounting for the reflectivity of the GI mirror or ML, the time resolution of this type of design would be two to four times poorer than that of the direct design, or of order 100 - 200 ms. This time resolution might be acceptable for ITER, since ITER operates in steady state.

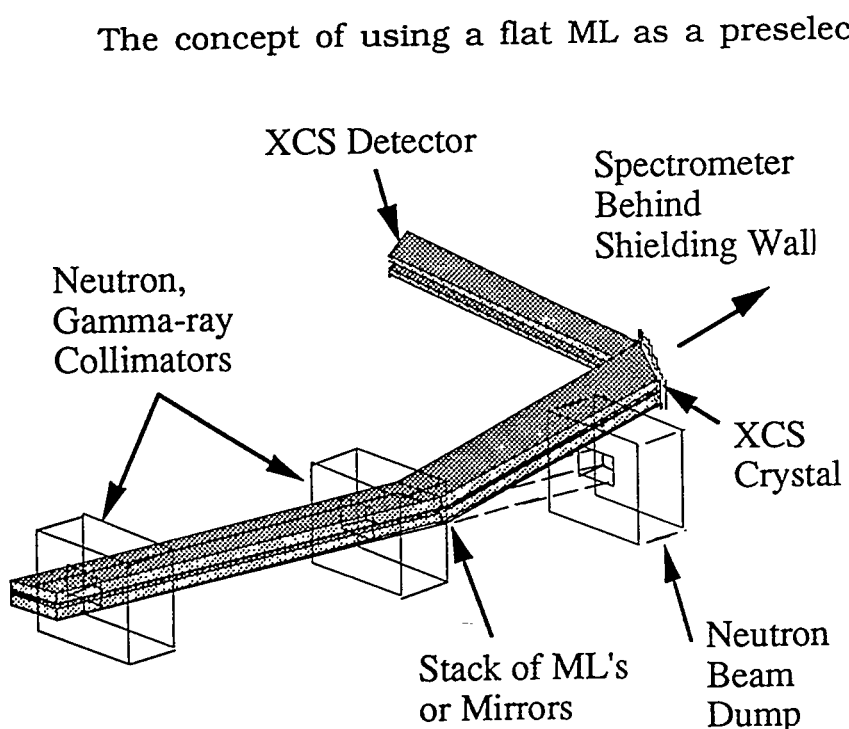


FIG. 9 Concept illustrating use of a stack of grazing-incidence x-ray mirrors or multilayers to deflect the x-ray beam to a curved-crystal spectrometer located behind the shielding wall of the ITER instrumentation room.

The concept of using a flat ML as a preselector for a high resolution XCS appears to be feasible; the intensity of the x-ray beam diffracted from the ML should be intense enough for T_i measurements. Since the rocking-curve width of multilayers is much broader than that of the quartz crystals typically used as diffraction elements for the XCS, the x rays coming from a ML tuned to the wavelength of interest should look like those from the plasma or reflected from a GI mirror, with the exception of a reduction in intensity by the ML peak reflectivity. The measured reflectivity of multilayers at 8 keV ranges from 30 to 50

percent with some values as high as 75 percent. Thus the intensity of x rays reflected from a ML mirror would be lower than that reflected from a GI mirror of equivalent projected area. However the projected area is proportional to the angle of incidence, which is larger by a factor of about 5 for a ML of d spacing 22 Å than for the GI mirror (at 13 keV), so the same length of ML mirror has a five times larger effective area than for a GI mirror. Thus, a single 40-cm long ML could replace the 5-mirror GI array. As discussed earlier, the bandpass of a standard ML ($E/\Delta E \sim 50-100$ at 8 keV) is about the same as or somewhat less than the bandpass required to transmit uniformly the entire Doppler-broadened helium-like $K\alpha$ x-ray

line plus a small region of continuum for background subtraction. Since the Johann curved-crystal spectrometer selects different wavelengths from different points on the Rowland circle, which means different parts of the ML, it would be simple to tune the ML to the wavelength desired at different points by slightly tilting the aperture relative to the multilayer. This tilting would have the effect of varying the incidence angle across the ML to satisfy the Bragg relation at all points. Otherwise, the bandwidth of the ML could be broadened slightly if required by slightly varying the layer spacing either laterally or with depth. Thus, the ML mirror appears to be a good candidate to remove the XCS from the direct neutron beam. The major advantage is that the angle of incidence and the deflection would be about five times larger than that of a GI mirror at 13 keV, so a single deflection is quite adequate to enable the neutron beam to clear the spectrometer.

Recent estimates of the radiation fluxes in the region inside the biological shield suggest that x-ray optics could survive for tens of thousands of hours of ITER operation in this region. The radiation flux onto the ITER blanket should be of order a few times 10^{14} particles $\text{cm}^{-2} \text{s}^{-1}$. The reduction due to the blanket is estimated to be of order 10^{-3} , and that resulting from a 2-m thick shield/collimator outside the vacuum vessel is estimated to be at least another factor of 10^{-3} . Thus, if such shields are placed outside the port covers in each bay, the ambient flux density inside the biological shield should be of order 10^9 $\text{cm}^{-2} \text{s}^{-1}$. The flux density streaming through a 1×10 cm^2 penetration in the 2-m thick plug would be of order 10^{11} $\text{cm}^{-2} \text{s}^{-1}$. Thus, with a damage threshold of 10^{18} cm^{-2} , the optic could last for of order 10^4 hours of operation at maximum power.

The capillary bundle x-ray light pipes appear not to be compatible with the XCS concept, because the curved crystal subtends a much larger angle at the focal point than the divergence of x rays from the capillary bundles, as illustrated in Fig. 6.

Recent developments in cryogenic x-ray bolometers suggest the possibility of eventually using these devices for ion temperature measurement without preselector optics. Arrays of order 100 elements (in a 1 cm^2 area) would be required to achieve the necessary count rates; the achievable rates are currently about 100 counts per second per detector. These rates might be increased to 1000 counts per second per detector. A program to evaluate semiconductor thermistors which might eventually be developed into such microbolometer arrays has been initiated.¹⁵ The present energy resolution (20 eV FWHM at 6 keV) is more than adequate for the PHA, but a factor of 1/20 reduction in the linewidth is necessary for replacing the XCS. Achievement of this improvement in energy resolution is theoretically possible. An x-ray/neutron aperture of about 0.5 cm diameter at ITER would reduce the Kr $K\alpha$ x-ray flux onto the detector 20 m away to the desired $\sim 10^5 \text{ s}^{-1}$ (for a Kr concentration of about 10^{-4}). The accompanying neutron flux density would be of the same magnitude to 10 times higher. However, since both the neutron and gamma-ray (>100 keV) interaction probabilities in the 7-mm thick Sn sensor are two to three

orders of magnitude smaller than that of the 13-keV x rays, the radiation background should be tolerable (See Fig. 10). To achieve these theoretical interaction ratios, one must be careful to minimize the contributions to the detector count rate from secondary radiation or electrons in the more massive material surrounding the sensor. Since the sensor is made of Sn, it should have a neutron damage threshold well above 10^{16} n cm⁻², although this number should be checked.. The Ge thermistor on the back of the Sn sensor has been neutron-transmutation doped to a neutron fluence of 10^{18} n cm⁻², followed by annealing at high temperature to remove neutron damage effects. It is expected that the thermistor might tolerate a fluence about 10^{13} neutrons/cm² before their performance deteriorates.¹⁵ This number is about three or four orders of magnitude higher than the damage thresholds of silicon and germanium x-ray detectors,^{8,31,32} and would correspond to about 100 - 1000 hours of operation of ITER at the expected neutron flux densities onto the detector of $10^6 - 10^7$ cm⁻² s⁻¹. After damage occurs the detectors could be annealed or replaced. If this lifetime is too short, the microbolometer array could be used in conjunction with a small GI or ML mirror and could, thus, operate for an indefinite time without neutron damage. This sort of detector, whether used in the neutron beam or with reflective optics, would have the effect of greatly simplifying the ion temperature measurements for more than one reason. The XCS is (1) very large and cumbersome, resulting in a requirement for a lot of space; it (2) must have the entrance and exit arms at a specific angle for a given crystal and x-ray energy, leading to the need to make difficult adjustments to the angles and selection of crystal (of which there is a limited selection available) to tune to the wavelengths of x rays from different ions; (3) the throughput is low, so that a relatively large aperture, crystal, and detector must be used, resulting in higher neutron streaming into the diagnostic area; and (4) it requires a large area position-sensitive detector which must be carefully shielded from stray nuclear radiation. In contrast, the microbolometer

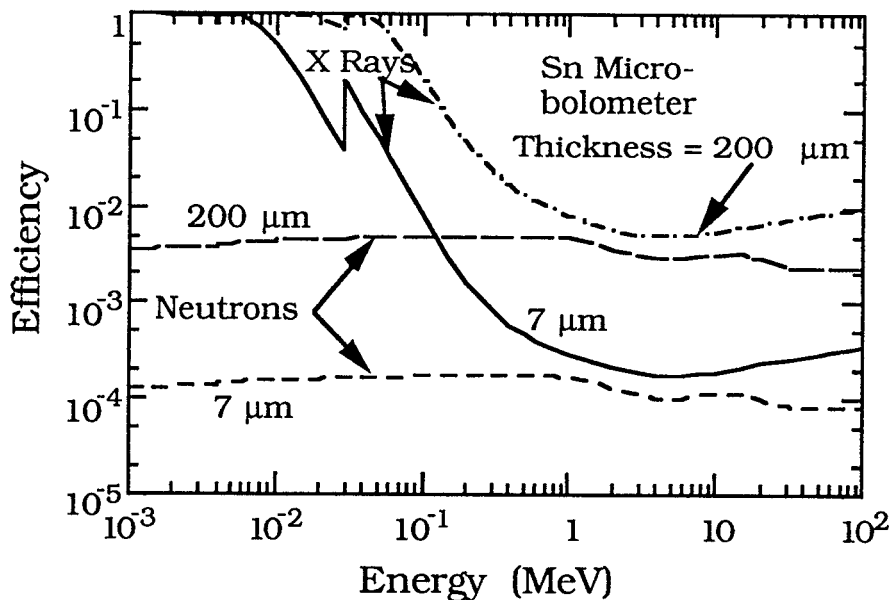


FIG. 10 Efficiencies for stopping x/γ rays and neutrons by Sn microbolometers of thickness 7 and 200 μm.

is, in principle small (although it does have the encumbrance of the sub-Kelvin refrigerator); has high efficiency and thus requires a small solid angle; is very insensitive to nuclear radiation; and has a broad bandwidth allowing it to measure x rays from any ions that may be in the plasma. One would simply insert an appropriate x-ray filter to remove the intense continuum radiation below the energy of the x-ray line of interest.

V. Broad-Band X-Ray Spectroscopy

The broad band spectroscopy for impurity measurement, electron-temperature measurement, and measurement of nonthermal electron distributions has historically been done by the soft x-ray PHA.³³ Also higher energy pulse-height or energy-dispersive spectrometers with good efficiency in the 50 keV to 1 MeV region have been used to obtain information on nonthermal electron distributions generated by RF-induced current drive in tokamaks.⁵ With present-day detectors neither of these systems could function usefully with the detectors viewing the plasma directly, even if the apertures were made very long to provide a similar solid angle for the neutrons as that for x rays. Thus, either additional x-ray optics must be used, or alternative detectors with low neutron/gamma response and high radiation-damage thresholds must be adopted.

The only presently known viable x-ray optical elements for broad-band PHA type diagnostics for electron temperature measurement or studies of non-thermal electron distribution functions are the GI mirror and the graded-d multilayers or supermirrors.^{21,22} The high energy cutoff of the capillary bundle (about 15 keV) is too low to be useful for nonthermal electron studies at ITER electron temperatures; furthermore, the PHA system is not fully compatible with the capillary bundle type preselector because the soft x-ray PHA usually has for some channels a smaller solid angle than the geometric angle of the capillary pores. In addition, to extend the energy to the range near 50 keV, two or three reflections would have to be used for the GI mirrors; it is not known whether GI mirrors would be useful at energies above 50 keV. It is known that supermirrors can have usable reflectivity (30 - 60 percent) for x rays from 15 to 70 keV at an angle near 3 mrad. For such a small angle, the deflection at 10 m may not be large enough to enable the exit collimator to clear the neutron beam. Additional optimization studies need to be done to investigate the bandpass at slightly larger angles, or alternatively to improve the high-energy efficiency (30 percent at 3 mrad) at somewhat smaller angles so that the high-energy efficiency for a double reflection is not too small to be acceptable. A 0.8 cm x 20 cm long mirror located 7 m from a 0.8 x 0.7 cm² aperture at ITER would provide the same $V\Omega$ product as the soft x-ray PHA on TFTR. A supermirror would need to be twice as long or both the aperture and mirror would need to be 50 percent wider to compensate for the low reflection efficiency at 70 keV. Since the PHA concept needs three detectors to avoid pileup distortions of the continuum spectrum, if the mirror width were chosen to be somewhat larger than the width of the aperture, then a small-

angle fan-shaped beam could be imaged onto three, in-line detectors at the exit end of the exit collimator.

For general x-ray spectroscopy on ITER for impurity monitoring, either a grazing-incidence mirror or capillary bundle optic would result in enough x-ray intensity in a reduced-radiation area to permit narrow-band crystal spectroscopy. The bandwidth would be limited, for a flat crystal, by the small angular range of x rays emanating from the optic. A convex curved-crystal with a position-sensitive detector could be used to provide a broader spectral bandwidth, with some loss in signal relative to that from a flat crystal because of the smaller crystal area used for each wavelength bin. We will not consider designs of such instruments in the present paper.

The x-ray microbolometers offer a potential alternative to current techniques for both broad-band and high resolution x-ray spectroscopy on tokamaks, and may not require x-ray optical elements to remove the detector from the neutron beam. At present, the energy resolution is about 20 eV (measured at 6 keV, but should be independent of energy), and the count rates per detector are about 100 per second. If arrays of about 100 such detectors can be developed and the individual rates can be increased to 1000 s^{-1} , this detector could be used in broad-band x-ray spectrometers for impurity measurement or measurement of impurity charge-state distributions.

VI. Discussion and Conclusions

Virtually all the conventional tokamak x-ray diagnostics can be adapted to the harsh radiation environment of ITER. For the XCS this adaptation means careful collimation and restriction of the neutron/gamma-ray beam falling onto the crystal and careful collimation and shielding of the detector from ambient and streaming radiation; for the XIS and PHA systems, it means addition of suitably designed x-ray optical elements or deflectors and careful collimation of the neutron beam and the viewing region of the detector or spectrometer, as well as shielding of the detector. The penetrations required in the radiation shield near ITER to view the x-ray emission are relatively small, ranging from about 1 cm^2 for the broad-band photon-counting spectroscopy and $1 \times 10 \text{ cm}^2$ for a chord of the XIS and XCS systems. The radiation levels at the x-ray optical elements for the aperture sizes required for useful signals are quite acceptable. Several thousands of hours of life are expected at full power. All of the designs considered in this report were based on a calculation of neutron scattering from an x-ray mirror which predicted a necessary lateral displacement of the x-ray beam from the neutron beam of 7 cm at a distance of 10 m in order to provide adequate reduction of the neutron background. This deflection requirement, however, was calculated for a fast-fluctuation-XIS type application, where the S/N needs to be large to enable measurement of small fluctuations (~ 1 percent) with good time resolution (1 - 10 μs). For both the XCS and the PHA, a smaller degree of reduction of the radiation

background may be acceptable, and, hence, a smaller angle of deflection may be acceptable. For the XCS this possibility is certainly acceptable, since the detector is already well removed from the neutron/gamma-ray beam which impinges onto the crystal. For the PHA, from a S/N standpoint, the lower level of isolation from the radiation beam is almost certainly acceptable; since (1) the typical few mm thick Si(Li) or Ge detectors have a smaller efficiency (~ 10 percent) for neutrons and MeV gamma rays than for soft x rays (~100 percent); (2) the surface brightness of the continuum x rays from ITER in the energy range above 30 keV (for $T_e = 30$ keV) is about the same as that of the neutron + gamma-ray brightness; and (3) only a fraction (~ 25 percent for Si) of the response to the nuclear radiation falls in the region of interest. Thus, for the PHA, a tenfold reduction in the nuclear component of the radiation makes measurements realistic. The more serious issue for the presently used PHA detectors is radiation damage due to the fast neutrons scattered from the deflector, since the thresholds for damage are of order 10^9 and 10^{10} for Ge and Si(Li) detectors,^{31,32} respectively. To enable PHA T_e measurements, lower-resolution, more radiation hard detectors might be used, such as proportional counters or NaI crystals.

At this time no attempt has been made to study techniques to deflect harder x-ray beams ($E > 100$ keV) for studies of RF-driven, non thermal electron distributions. The necessary additional x-ray optics will complicate the instrument designs, make them more bulky and expensive, and in some cases limit the range of applicability. For example, conventional soft x-ray PHA systems can measure x rays from 1 to 100 keV with almost 100 percent efficiency, whereas, with present technology it might be difficult to maintain high efficiency and broad bandwidth with grazing-incidence reflective optics for energies above about 70 keV. One approach for x-ray telescopes at lower energies (6 - 8 keV) has been to combine ML reflectors with GI reflectors to enhance the high-energy throughput.

The x-ray crystal spectrometer studies of instrument designs for measuring the ion temperature in the ITER core by Doppler broadening of krypton $K\alpha$ x rays have been augmented by several experimental and theoretical studies.^{11,27,28,34,35} As a catalyst, it had been suggested that edge radiative cooling of ITER by injection of high-Z elements might aid in limiting the power flow to the divertor and more uniformly distributing the power loading onto the plasma-facing components.³⁵ The MIST impurity transport code³⁶ was used to calculate the expected radial charge-state distributions and $K\alpha$ emissivity for iron and krypton; krypton had the advantage in that the helium-like and hydrogen-like charge states of the lower-Z iron began to burn out at the high electron temperatures of about 30 keV eventually expected in ITER. Also, it was shown that reasonably small, non perturbing concentrations of krypton ($n_{Kr}/n_e = 10^{-4}$) could both produce the required radiative cooling and emit an adequate x-ray intensity that would not be drowned out by neutron and gamma-ray noise, if the XCS instrument were properly shielded. Experiments on TFTR with krypton gas puffing showed that XCS measurements of Kr $K\alpha$ spectra could be used to

measure the ion temperature.^{27,28} In addition, it was shown that the MIST code correctly predicted the measured radiated power from TFTR when the krypton concentrations, as measured by the absolutely-calibrated PHA diagnostic, were entered into the input data. Furthermore, earlier comparisons of the iron concentration in TFTR plasmas, as determined from the helium-like resonance line measured by the XCS, showed reasonable agreement with that measured by the PHA. Differences were typically in the range 20 - 30 percent. For the XCS measurements Eq. 2 was used along with published values of the quartz crystal integrated reflectivities³⁷ and MIST-code simulations. These comparisons give us confidence that the published values of the integrated reflectivities can be used with confidence in Eq. 2. The TFTR krypton measurements, along with theoretical line-wavelength calculations, also showed that the normally-used helium-like resonance line is significantly broadened by nearby satellite lines at low electron temperatures (5-6 keV), but that the forbidden line is unblended and can be used for ion-temperature measurements. Other precision measurements³⁵ of the wavelengths and excitation rates of the multitude of lines in the neighborhood of the diagnostic lines have begun to provide further guidance and confidence in use of these lines as a reliable ion-temperature diagnostic.

Acknowledgments

The authors gratefully acknowledge the support and helpful discussions with K. M. Young. Also acknowledged are helpful discussions with L.-P. Ku, A. S. Krieger, and K. Joensen. We thank Dr. A. S. Krieger and D. Parsignault for the glass-capillary bundle gain data plotted in Fig. 7.

References:

- ¹ Tokamak Physics Studies Using X-Ray Diagnostic Methods, K. W. Hill, M. Bitter, S. von Goeler, P. Beiersdorfer, E. Fredrickson, H. Hsuan, K. McGuire, N. R. Sauthoff, S. Sesnic, and J. E. Stevens in *Proceedings of the Course and Workshop on Basic and Advanced Fusion Plasmas, Diagnostic Techniques*, (Varenna (Como), Italy, September 1986), (Monotypia Franchin, Citta' di Castello, Italy and Office for Official Publications of the European Communities, Luxembourg, Belgium, 1987), edited by P. Stott, D. K. Akulina, G. G. Leotta, E. Sindoni, and C. Wharton, Vol. I, pp. 169-200
- ² Tokamak X-Ray Diagnostic Instrumentation, K. W. Hill, P. Beiersdorfer, M. Bitter, E. Fredrickson, S. von Goeler, H. Hsuan, L. C. Johnson, S-L. Liew, K. McGuire, V. Pare, N. R. Sauthoff, S. Sesnic, and J. E. Stevens, *Ibid.*, pp. 201-226.

- 3 Diagnostic Applications of the TFTR XIS System, K. McGuire, R. J. Colchin, E. Fredrickson, K. Hill, L. C. Johnson, W. Morris, V. Pare, N. Sauthoff, and S. von Goeler, *Rev. Sci. Instrum.* **57**, 2136-2138 (August 1986)
- 4 Tokamak Fusion Test Reactor Prototype X-Ray Pulse-Height Analyzer Diagnostic, K. W. Hill, M. Bitter, M. Diesso, L. Dudek, S. von Goeler, S. Hayes, L. C. Johnson, G. Renda, S. Sesnic, N. R. Sauthoff, F. H. Tenney, and K. M. Young, *Rev. Sci. Instrum.* **56**, 840-842 (May 1985)
- 5 Angular Distribution of the Bremsstrahlung Emission During Lower-Hybrid Current Drive on PLT, S. von Goeler, J. E. Stevens, S. Bernabei, M. Bitter, T. K. Chu, P. C. Efthimion, N. J. Fisch, W. M. Hooke, K. W. Hill, J. C. Hosea, F. C. Jobes, C. F. F. Karney, E. Mazzucato, J. A. Mervine, E. B. Meservey, R. W. Motley, P. G. Roney, S. Sesnic, K. Silber, and G. Taylor, *Nucl. Fusion* **25**, 1515-1528 (November 1985)
- 6 Doppler-Broadening Measurements of X-Ray Lines for Determination of the Ion Temperature in Tokamak Plasmas, M. Bitter, S. von Goeler, R. Horton, M. Goldman, K. W. Hill, N. R. Sauthoff, and W. Stodiek, Princeton University, Plasma Physics Laboratory Report PPPL-1490 (November 1978) 15 pp., *Phys. Rev. Lett.* **42**, 304-307 (January 1979)
- 7 The TFTR High-Resolution Bragg X-Ray Spectrometer, K. W. Hill, M. Bitter, M. Tavernier, M. Diesso, S. von Goeler, G. Johnson, L. C. Johnson, N. R. Sauthoff, N. Schechtman, S. Sesnic, F. H. Tenney, and K. M. Young, *Rev. Sci. Instrum.* **56**, 1165-1168 (June 1985)
- 8 X-Ray Diagnostics for TFTR, S. von Goeler, K. W. Hill, M. Bitter, C. Clifford, E. Fredd, M. Goldman, L. C. Johnson, L. P. Ku, E. Moshey, G. Renda, N. R. Sauthoff, S. Sesnic, F. H. Tenney, and K. M. Young, Princeton University, Plasma Physics Laboratory Report PPPL-1958 (December 1982) 37 pp., *Proceedings of the Course, Diagnostics for Fusion Reactor Conditions, Varenna, Italy, September 1982, Vol. I, pp. 69-85*
- 9 F. Bombarda, R. Giannella, E. Kallne, G. J. Tallents, F. Bely-Dubau, P. Faucher, M. Cornille, J. Dubau, and A. H. Gabriel, *Phys. Rev.* **A37**, 504 (1988)
- 10 R. Barnsley, U. Schumacher, E. Kallne, H. W. Morsi, and G. Rupprecht, *Rev. Sci. Instrum.* **62**, 889 - 898 (1991); Design Study for the JET Diagnostic System Number 12.7, W. Engelhardt, J. Fink, G. Fussmann, H. Krause, H. -B. Schilling, and U. Schumacher, IPP-JET Report No. 5, March 1982.
- 11 ITER X-Ray Diagnostic Studies, K. W. Hill, K. M. Young, M. Bitter, S. von Goeler, H. Hsuan, R. Hulse, L.-P. Ku, B. C. Stratton, A. S. Krieger, D. Parsignault, and E. D. Franco, *Rev. Sci. Instrum.* **63**, 5032-5034 (October 1992)

-
- 12 ITER X-Ray Fluctuation Diagnostic Possibilities, K. W. Hill, M. Bitter, S. von Goeler, H. Hsuan, and K. M. Young, Princeton Plasma Physics Laboratory report number PPPL-3008, (September, 1994)
 - 13 Thermal Detectors as X-Ray Spectrometers, S. H. Moseley, J. C. Mather, D. McCammon, J. Appl. Phys. **56**, 1257 (1984)
 - 14 Microcalorimeters for Broad Band High Resolution X-Ray Spectral Analysis, Mark LeGros, Eric Silver, Norman Madden, Jeffrey Beeman, Frederick Goulding, Donald Landis, and Eugene Haller, Lawrence Livermore National Laboratory Report UCRL-JC-116343, to be published in Nucl. Instrum. Meth. in Phys. Research.
 - 15 E. Silver, Private communication.
 - 16 Zeff Profiles Measured by Visible and Soft X-Ray Bremsstrahlung Arrays in TFTR, H. Park, H. Adler, and K. W. Hill, 10th Topical Conference on High Temperature Diagnostics, 8-12 May, 1994, Rochester, New York, to be published in Rev. Sci. Instrum.
 - 17 X-Ray Mirror Reflectivities from 3.8 to 50 keV, Part II - Pt, Si, and Other Materials, D. H. Bilderback and S. Hubbard, Nucl. Instrum. Methods, **195**, 91 (1982).
 - 18 Grazing Incidence Imaging from 10 to 40 keV, Martin Elvis, Daniel G. Fabricant, and Paul Gorenstein, SPIE Vol. **830**, 296(1988).
 - 19 Manufacture, Structure, and Performance of W/B4C Multilayer X-Ray Mirrors, A. F. Jankowski and D. M. Makowiecki, in *X-Ray Multilayers for Diffractometers, Monochromators, and Spectrometers*, Ed. Finn E. Christensen, (SPIE, Bellingham, WA 1988), Vol. 984, p. 64.
 - 20 Influence of Electrical Isolation on the Structure and Reflectivity of Multilayer Coatings Deposited on Dielectric Substrates, Georgy Gutman, John Keem, Jim Wood, Charles Tarrío, and Richard Watts, Applied Optics **32**, 6981 (December 1993).
 - 21 Medium-Sized Grazing-Incidence High-Energy X-Ray Telescopes Employing Continuously Graded Multilayers, K. D. Joensen, F. E. Christensen, H. W. Schnopper, P. Gorenstein, J. Susini, P. Høghøj, R. Hustache, J. Wood, and K. Parker, Proc. SPIE , **1736**, p. 236 (1992).
 - 22 Broad-Band Focusing of Hard X-Rays using a Supermirror, Peter Hoghoj, Eric Ziegler, Jean Susini, Andreas K. Freund, Karsten Dan Joensen, and Paul Gorenstein, in Physics of X-Ray Multilayer Structures, 1994 Technical Digest Series (Optical Society of America, 1994), Vol VI, p. 142.
 - 23 Layered Synthetic Microstructure X-Ray Mirror Focusing Instrument:

-
- Bent Silicon Wafer Substrate, J. A. Penkethman, *Optical Engineering* **27**, 99 (1988).
- 24 Grazing-Incidence Fe-Line Telescopes using W/B₄C Multilayers, K. D. Joensen, P. Gorenstein, F. Christensen, and G. Gutman, in *Multilayer and Grazing-Incidence X-Ray/EUV Optics II*, (SPIE, Bellingham, WA 1993), Vol. 2011.
- 25 K. Joensen, private communication.
- 26 X-Ray Fiber Optics from 60 eV to 10 keV, D. Parsignault and A. S. Krieger, in *X-Ray Detector Physics and Applications*, edited by R. Hoover, (SPIE, Bellingham, WA 1992), Vol. 1736.
- 27 Spectra of Heliumlike Krypton from Tokamak Fusion Test Reactor Plasmas, M. Bitter, H. Hsuan, C. Bush, S. Cohen, C. J. Cummings, B. Grek, K. W. Hill, J. Schivell, M. Zarnstorff, P. Beiersdorfer, A. Osterheld, A. Smith, and B. Fraenkel, *Phys. Rev. Lett.* **71**, 1007 (1993).
- 28 X-Ray Spectra of Heliumlike Krypton as a Potential Ion-Temperature Diagnostic for the International Thermonuclear Experimental Reactor (ITER), M. Bitter, H. Hsuan, K. W. Hill, R. Hulse, M. Zarnstorff, and P. Beiersdorfer, *Atomic and Plasma-Material Interaction Processes in Controlled Thermonuclear Fusion*, (Elsevier Science Publishers, 1993), edited by R. K. Janev and H. W. Drawin, pp. 119-133.
- 29 X-Ray Optics for ITER Spectrometer, V. A. Bryzgunov, A. B. Gil'varg, and A. N. Svetchkopal, Russian Research Center Kurchatov Institute report number IAE-5645/14 (Moscow 1993), presented at the Sixth National Topical Conference on High Temperature Plasma Diagnostics, St. Petersburg, May 26 1993.
- 30 Numerical Study of the Imaging Properties of Doubly-Focusing Crystals, M. Bitter, B. Fraenkel, K. W. Hill, H. Hsuan, and S. von Goeler, paper 3.22, presented at the 10th Topical Conference on High Temperature Plasma Diagnostics, 8-12 May, 1994, Rochester, N. Y, to be published in *Rev. Sci. Instrum.*
- 31 Y. M. Liu and J. A. Coleman, *IEEE Trans. Nucl. Sci.* **NS-19**, p. 346 (1972)
- 32 F. Goulding and R. H. Pehl, *IEEE Trans. Nucl. Sci.* **NS-22**, p. 149 (1975)
- 33 Studies of Impurity Behavior in TFTR, K. W. Hill, M. Bitter, N. L. Bretz, M. Diesso, P. C. Efthimion, S. von Goeler, J. Kiraly, A. T. Ramsey, N. R. Sauthoff, J. Schivell, and S. Sesnic, *Nucl. Fusion* **26**, 1131-1141 (August 1986)

- 34 C. J. Cummings, S. Cohen, R. Hulse, D. E. Post, and M. Redi, *J. Nucl. Mater.* **176 & 177**, 916, (1990).
- 35 Spectroscopy and Atomic Physics in EBIT and SuperEBIT, P. Beiersdorfer, M. Bitter, M. Chen, V. Decaux, S. Elliott, S. Kahn, D. Knapp, R. Marrs, A. Osterheld, D. Vogel, and K. Widmann, UCRL-JC-114373 (December, 1993).
- 36 Hulse, R. A, *Nucl. Technol./Fusion* **3**, 259 (1983)
- 37 Crystals for Astronomical X-Ray Spectroscopy, Anthony Burek, *Space Science Instrum.* **2**, 53 (1976).

EXTERNAL DISTRIBUTION IN ADDITION TO UC-420

Dr. F. Paoloni, Univ. of Wollongong, AUSTRALIA
 Prof. R.C. Cross, Univ. of Sydney, AUSTRALIA
 Plasma Research Lab., Australian Nat. Univ., AUSTRALIA
 Prof. I.R. Jones, Flinders Univ, AUSTRALIA
 Prof. F. Cap, Inst. for Theoretical Physics, AUSTRIA
 Prof. M. Heindler, Institut für Theoretische Physik, AUSTRIA
 Prof. M. Goossens, Astronomisch Instituut, BELGIUM
 Ecole Royale Militaire, Lab. de Phy. Plasmas, BELGIUM
 Commission-European, DG. XII-Fusion Prog., BELGIUM
 Prof. R. Bouciqué, Rijksuniversiteit Gent, BELGIUM
 Dr. P.H. Sakanaka, Instituto Fisica, BRAZIL
 Prof. Dr. I.C. Nascimento, Instituto Fisica, Sao Paulo, BRAZIL
 Instituto Nacional De Pesquisas Espaciais-INPE, BRAZIL
 Documents Office, Atomic Energy of Canada Ltd., CANADA
 Ms. M. Morin, CCFM/Tokamak de Varennes, CANADA
 Dr. M.P. Bachynski, MPB Technologies, Inc., CANADA
 Dr. H.M. Skarsgard, Univ. of Saskatchewan, CANADA
 Prof. J. Teichmann, Univ. of Montreal, CANADA
 Prof. S.R. Sreenivasan, Univ. of Calgary, CANADA
 Prof. T.W. Johnston, INRS-Energie, CANADA
 Dr. R. Bolton, Centre canadien de fusion magnétique, CANADA
 Dr. C.R. James,, Univ. of Alberta, CANADA
 Dr. P. Lukác, Komenského Univerzita, CZECHO-SLOVAKIA
 The Librarian, Culham Laboratory, ENGLAND
 Library, R61, Rutherford Appleton Laboratory, ENGLAND
 Mrs. S.A. Hutchinson, JET Library, ENGLAND
 Dr. S.C. Sharma, Univ. of South Pacific, FIJI ISLANDS
 P. Mähönen, Univ. of Helsinki, FINLAND
 Prof. M.N. Bussac, Ecole Polytechnique,, FRANCE
 C. Mouttet, Lab. de Physique des Milieux Ionisés, FRANCE
 J. Radet, CEN/CADARACHE - Bat 506, FRANCE
 Prof. E. Economou, Univ. of Crete, GREECE
 Ms. C. Rinni, Univ. of Ioannina, GREECE
 Preprint Library, Hungarian Academy of Sci., HUNGARY
 Dr. B. DasGupta, Saha Inst. of Nuclear Physics, INDIA
 Dr. P. Kaw, Inst. for Plasma Research, INDIA
 Dr. P. Rosenau, Israel Inst. of Technology, ISRAEL
 Librarian, International Center for Theo Physics, ITALY
 Miss C. De Palo, Associazione EURATOM-ENEA , ITALY
 Dr. G. Grosso, Istituto di Fisica del Plasma, ITALY
 Prof. G. Rostangni, Istituto Gas Ionizzati Del Cnr, ITALY
 Dr. H. Yamato, Toshiba Res & Devel Center, JAPAN
 Prof. I. Kawakami, Hiroshima Univ., JAPAN
 Prof. K. Nishikawa, Hiroshima Univ., JAPAN
 Librarian, Naka Fusion Research Establishment, JAERI, JAPAN
 Director, Japan Atomic Energy Research Inst., JAPAN
 Prof. S. Itoh, Kyushu Univ., JAPAN
 Research Info. Ctr., National Instit. for Fusion Science, JAPAN
 Prof. S. Tanaka, Kyoto Univ., JAPAN
 Library, Kyoto Univ., JAPAN
 Prof. N. Inoue, Univ. of Tokyo, JAPAN
 Secretary, Plasma Section, Electrotechnical Lab., JAPAN
 Dr. O. Mitarai, Kumamoto Inst. of Technology, JAPAN
 Dr. G.S. Lee, Korea Basic Sci. Ctr., KOREA
 J. Hyeon-Sook, Korea Atomic Energy Research Inst., KOREA
 D.I. Choi, The Korea Adv. Inst. of Sci. & Tech., KOREA
 Prof. B.S. Liley, Univ. of Waikato, NEW ZEALAND
 Inst of Physics, Chinese Acad Sci PEOPLE'S REP. OF CHINA
 Library, Inst. of Plasma Physics, PEOPLE'S REP. OF CHINA
 Tsinghua Univ. Library, PEOPLE'S REPUBLIC OF CHINA
 Z. Li, S.W. Inst Physics, PEOPLE'S REPUBLIC OF CHINA
 Prof. J.A.C. Cabral, Instituto Superior Tecnico, PORTUGAL
 Prof. M.A. Hellberg, Univ. of Natal, S. AFRICA
 Prof. D.E. Kim, Pohang Inst. of Sci. & Tech., SO. KOREA
 Prof. C.I.E.M.A.T, Fusion Division Library, SPAIN
 Dr. L. Stenflo, Univ. of UMEA, SWEDEN
 Library, Royal Inst. of Technology, SWEDEN
 Prof. H. Wilhelmson, Chalmers Univ. of Tech., SWEDEN
 Centre Phys. Des Plasmas, Ecole Polytech, SWITZERLAND
 Bibliotheek, Inst. Voor Plasma-Fysica, THE NETHERLANDS
 Asst. Prof. Dr. S. Cakir, Middle East Tech. Univ., TURKEY
 Dr. V.A. Glukhikh, Sci. Res. Inst. Electrophys. Apparatus, USSR
 Dr. D.D. Ryutov, Siberian Branch of Academy of Sci., USSR
 Dr. G.A. Eliseev, I.V. Kurchatov Inst., USSR
 Librarian, The Ukr.SSR Academy of Sciences, USSR
 Dr. L.M. Kovrizhnykh, Inst. of General Physics, USSR
 Kernforschungsanlage GmbH, Zentralbibliothek, W. GERMANY
 Bibliothek, Inst. Für Plasmaforschung, W. GERMANY
 Prof. K. Schindler, Ruhr-Universität Bochum, W. GERMANY
 Dr. F. Wagner, (ASDEX), Max-Planck-Institut, W. GERMANY
 Librarian, Max-Planck-Institut, W. GERMANY